PHYSICAL REVIEW B **92**, 041108(R) (2015)

Route to room-temperature ferromagnetic ultrathin $SrRuO_3$ films

Liang Si, Zhicheng Zhong,* Jan M. Tomczak, and Karsten Held
Institute of Solid State Physics, Vienna University of Technology, A-1040 Vienna, Austria
(Received 10 March 2015; revised manuscript received 19 June 2015; published 9 July 2015)

Experimental efforts to stabilize ferromagnetism in ultrathin films of transition metal oxides have so far failed, despite expectations based on density functional theory (DFT) and DFT+U. Here, we investigate one of the most promising materials, $SrRuO_3$, and include correlation effects beyond DFT by means of dynamical mean-field theory. In agreement with experiment, we find an intrinsic thickness limitation for metallic ferromagnetism in $SrRuO_3$ thin films. Indeed, we demonstrate that the realization of ultrathin ferromagnetic films is out of reach of standard thin-film techniques. Proposing charge carrier doping as an alternative route to manipulate thin films, we predict room-temperature ferromagnetism in electron-doped $SrRuO_3$ ultrathin films.

DOI: 10.1103/PhysRevB.92.041108 PACS number(s): 73.61.−r, 31.15.A−, 31.15.V−, 73.50.−h

Introduction. Thin films and heterostructures of the 4*d* perovskite $SrRuO_3$ (SRO) are intensively studied and used, in particular, as gate electrodes for novel oxide-based electronic devices [1,2]. The reason for this is that SRO is a conductor with good thermal properties [3] and high chemical stability, allowing for epitaxial growth on various substrates, as well as combining with other perovskite-based materials to form complex heterostructures [4,5]. In the bulk, SRO is a ferromagnetic (FM) metal with, for a 4*d* oxide, a remarkably high Curie temperature, $T_C = 160$ K, and an experimental magnetic moment in the range of 0.8–$1.6\mu_B$ [6–9]. SRO has further attracted fundamental research interests regarding, among others, magnetic monopoles [10], non-Fermi liquids [11], spin freezing [12], and the debate on itinerant [13] versus localized magnetism [14].

However, the FM moment and Curie temperature become dramatically suppressed below a sample thickness of four unit cells [15–18], and eventually single unit cell SRO films turn antiferromagnetic (AF) and insulating [17,18]. This has led to the pertinent question of whether there is a fundamental thickness limit for ferromagnetism [18], and concerted efforts to stabilize ferromagnetism in ultrathin SRO films by compressive and tensile strain or capping layers [19,20]. However, hitherto ferromagnetism in single unit cell films remains unattainable for SRO or other oxide materials, even in a heterostructured setup.

On the theoretical side, previous attempts to understand the electronic structure and the transition to an AF insulator resorted to density functional theory (DFT) and the static mean-field DFT+U approach. The former failed to reproduce the transition [21], while the latter found a transition to an AF insulating state below four layers when assuming an artificial RuO_2 terminated surface [22], while, experimentally, samples are found to have a SrO termination [5]. DFT+U further predicted a spin-polarized highly confined half-metallic state for an SRO monolayer when either sandwiched with $SrTiO_3$ (STO) [19] or grown on a strained STO substrate [20]. However, such a state could not be confirmed in experiment [23]. The apparent discrepancy between experiments and results from standard band-structure methods calls for a more sophisticated treatment of electronic correlation effects. Indeed, already in the bulk, SRO displays signatures of electronic correlations, such as many-body satellites in photoemission or the violation of the Ioffe-Regel limit in the resistivity [8,24]. Hence, SRO is to be considered an—at least—moderately correlated system. Note that dimensional reduction/geometric constraints in thin films can be expected to further enhance electronic correlations.

For a better and unbiased treatment of these correlation effects in various SRO films and heterostructure setups, we employ realistic DFT+dynamical mean-field theory (DMFT) [25–29] calculations. Our main findings are as follows: (1) Both the SRO monolayer and bilayer are AF insulators. (2) We demonstrate that standard thin-film manipulation techniques such as strain and surface capping can neither restore ferromagnetism nor metallicity to a SRO monolayer; interestingly, we find that surface capping pushes the AF insulator towards a paramagnetic (PM) insulator. (3) With insight regarding the microscopic origin for the transition, we identify carrier doping as the best option to generate FM properties that are on par with those of the bulk. We find the FM moments of doped SRO films to be stable even at room temperature, heralding a great potential for technological applications.

Method. We use the experimental orthorhombic crystal structure of SRO [30] for the various setups of bulk, films, and heterostructures. In the films and heterostructure both the internal positions and lattice constant are relaxed; the in-plane lattice constants in films are fixed to our optimized value, 3.95 Å, of STO. Figure 1 exemplary shows the SRO monolayer grown on four layers of a STO substrate. The atomic relaxations are carried out with the VASP program package [32,33] using the Perdew-Burke-Ernzerhof (PBE) functional [34]. For the optimized atomic positions, we subsequently perform WIEN2K [35] electronic structure calculations with the modified Becke-Johnson (mBJ) exchange [36] and PBE correlation functional [37], and a Wannier projection onto maximally localized [38] t_{2g} Wannier functions [39] using the WIEN2WANNIER program package [40]. This t_{2g} Hamiltonian is supplemented by a local Kanamori interaction and solved within DMFT using WIEN2DYNAMICS [41], employing a hybridization expansion continuous-time quantum Monte Carlo (CTQMC) algorithm [42]. For the Coulomb interaction strengths, we adopt a Hund's exchange ($J = 0.3$ eV), and intraorbital ($U = 3.0$ eV) and interorbital Coulomb repulsion ($U' = 2.4$ eV). These values consistently yield a FM metallic state for orthorhombic bulk SRO. Performing constrained

*Corresponding author: zhicheng.zhong@ifp.tuwien.ac.at

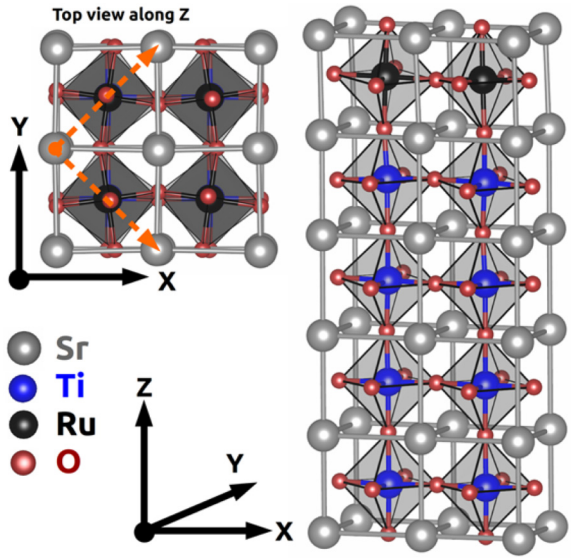

FIG. 1. (Color online) Right: Structure of a SRO monolayer grown on four layers of STO. Upper left: Top view of the same structure. The indicated $\sqrt{2} \times \sqrt{2}$ supercell was adopted for allowing AF ordering in each RuO_2 layer. Lower left: Atomic labels and coordinate system (figures drawn with the VESTA code [31]).

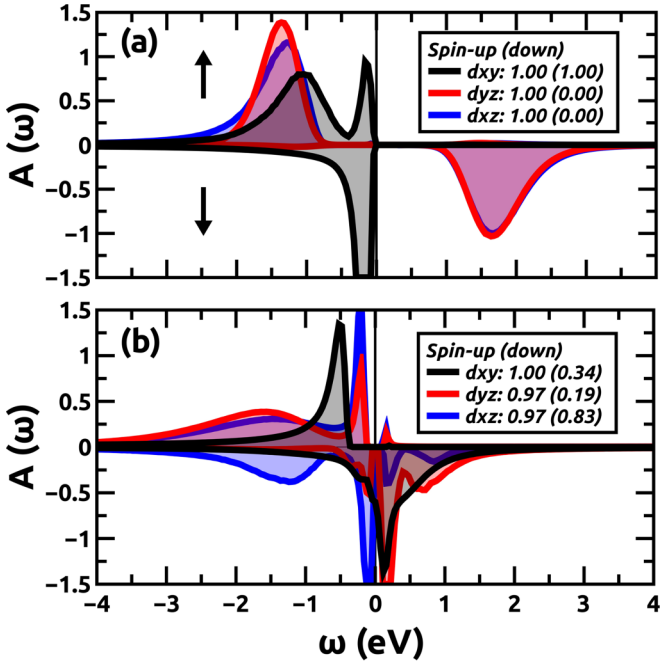

FIG. 2. (Color online) DFT+DMFT spectral functions of (a) the AF SRO monolayer on a STO substrate and (b) the FM doped (4.3 electrons/Ru) superlattice $(STO)_5:(SRO)_1$ at 150 K. Insets: Electronic occupations.

random phase approximation (cRPA) calculations [43], for a freestanding cubic SRO monolayer (along the lines of Ref. [44]), we find an only slightly enhanced value $U = 3.5$ eV, while $J = 0.3$ eV and $U' = 2.9$ eV.

Bulk $SrRuO_3$. The moderately correlated electronic structure of *bulk* SRO was successfully captured in both many-body perturbation theory [45] and realistic DMFT calculations [46,47]. Also, DFT calculations correctly predict that SRO is an itinerant ferromagnet with a moment ranging from $1.5\mu_B$ to $1.6\mu_B$ [8,48]; similar moments have also been obtained within DFT+DMFT [47,49]. Using DFT+DMFT, we indeed find orthorhombic bulk SRO to be a FM metal with orbital occupations of 0.908 (0.447), 0.866 (0.449), and 0.881 (0.449) for the majority (minority) spin of xy, yz, and xz orbitals at $T = 100$ K. This corresponds to a FM magnetic moment of $1.31\mu_B$. A $GdFeO_3$-type distortion in which the corner-sharing octahedra tilts around the y axis and rotates around the z axis lifts, in principle, the t_{2g} degeneracy. The effect on the crystal field and orbital occupations in orthorhombic SRO is, however, minute. Our DFT+DMFT finds SRO to be a PM metal above $T_C \sim 150$ K, which is close to the experimental Curie temperature of 160 K (cf. Fig. 3 below).

Thin films. We now consider SRO grown on STO, and study the evolution of the electronic structure when reducing the number of SRO layers. We find that FM is suppressed: The monolayer and bilayer SRO on STO are AF insulators, in congruence with experiments [18,23] that show a dramatic drop in the FM moment and an insulating behavior for four layers or lower [15–18,23]. Recent experiments [50] confirm the nonferromagnetic and insulating state in bilayer SRO, and yield photoemission spectra in good agreement with our theoretical results (see the Supplemental Material [51]). Indicative of an itinerant origin of ferromagnetism, the critical thicknesses of the magnetic and electronic transition coincide.

Figure 2(a) shows the spectral function of the monolayer. The system is gapped by $\sim$1.0 eV and displays a large orbital polarization: The xy orbital is fully filled, and the xy and xz orbitals are half filled and fully spin polarized, resulting in an AF moment of $\sim 2\mu_B$. This finding is supported by recent exchange bias measurements [17].

We note that for the particular case of the SRO monolayer, also the local density approximation (LDA)+U [20] can seemingly give a qualitatively correct picture, as the system is orbitally and spin polarized. However, the underlying physics is very different: When heating the monolayer above its Néel temperature within DMFT, the system remains insulating at noninteger filling [0.88 (0.88), 0.56 (0.56), and 0.56 (0.56) for the spin up (down) xy, yz, and xz orbitals at 1000 K]. This complex Mott physics [52] reveals that the AF insulating phase is beyond a simple Slater description, and thus not describable by LDA+U.

Physical origin of transition. Let us now investigate the microscopic origin of the FM-metal to AF-insulator transition. Whereas the crystal-field splitting is minute for the bulk, in the SRO monolayer the xy orbital is energetically lower than the yz and xz orbitals, because the surface breaks the crystal symmetry in the z direction (besides the bulklike orthorhombic distortion in the SRO layer, the surface relaxation causes surface O to move away from the topmost RuO_2 layer, while surface Sr moves toward it). This is already the case for the DFT Wannier Hamiltonian, but correlation effects boost the crystal-field splitting [52–54] of the SRO monolayer (see Table I in the Supplemental Material). Therewith, the xy orbital becomes essentially fully occupied, and the two remaining electrons occupy the yz and xz orbitals: The single-layer SRO

TABLE I. Magnetic and conductive states of bulk SRO, SRO monolayer (also under 0.5% compression and 0.5% tension), SRO bilayers, and $(STO)_5:(SRO)_1$ superlattice (capped monolayer), as obtained from spin-polarized DFT and DFT+DMFT calculations in comparison with experiment. FM-M: ferromagnetic metal; AF-I: antiferromagnetic insulator; NM-I: nonferromagnetic insulator (the magnetic nature of the experimental nonferromagnetic state has not yet been fully determined; the exchange bias behavior hints at antiferromagnetism [17]).

System	DFT	DMFT	Expt.
Bulk	FM-M	FM-M	FM-M [6]
Monolayer 100.5%	FM-M	AF-I	
Monolayer 100%	FM-M	AF-I	NM-I [17]
Monolayer 99.5%	FM-M	AF-I	
Bilayer	FM-M	AF-I	NM-I [15,50]
Superlattice	FM-M	AF-I	NM-I [23]
Hole-doped superlattice	FM-M	FM-M	
Electron-doped superlattice	FM-M	FM-M	

is an effective half-filled two-band system, favorable to AF order.

Tuning the properties of the SRO monolayer. The prime motivations for SRO-based thin films are the advantageous properties of the FM metallic *bulk*. However, the desired features, such as the magnetic moment, strongly decrease for thinner films and eventually ultrathin films become non-FM, in agreement with our calculations. A natural question is whether the bulk properties can be restored, at least partially, by tuning the geometry of the films.

First, we discuss the influence of straining or tensioning the monolayer. This can be realized experimentally by choosing an appropriate substrate. Indeed, previous DFT+U calculations [20] predicted a strain-induced FM half-metallic state for the SRO monolayer. DFT+DMFT, however, does not show any such tendency (see Table I), at least for realistic U values (see Table II in the Supplemental Material). Also, the effective crystal-field splitting Δ_{eff}, shown in Table I of the Supplemental Material, can only be tuned slightly through straining or tensioning.

Another way to influence the crystal-field splitting is through the deployment of capping layers. Here, we study the effect of capping the SRO monolayer with additional layers of STO. Specifically, we consider a $(STO)_5:(SRO)_1$ superlattice [19] consisting of five layers of STO alternating with a monolayer of SRO. This restores, at least partially, the hopping amplitudes in the out-of-plane direction. Compared to the SRO monolayer, the DFT crystal-field splitting, shown in Table I of Supplemental Material, is now much smaller (-0.05 eV), approaching the negligible value of the bulk. As a result, the t_{2g} orbital occupations are more balanced. However, this causes only a slight reduction of the AF magnetic moment [$1.92\mu_B$ at 150 K and $1.48\mu_B$ at 300 K—cf. Fig. 3(b)] with respect to the uncapped monolayer. Our finding of a non-FM insulating state with a gap of $\sim$1.0 eV for the capped monolayer is consistent with experiments [23,55], where it was concluded that SRO capped by STO leads to an insulator without a net moment. We note that previous DFT+U calculations [19] instead predicted a FM half metal, at variance with experiment.

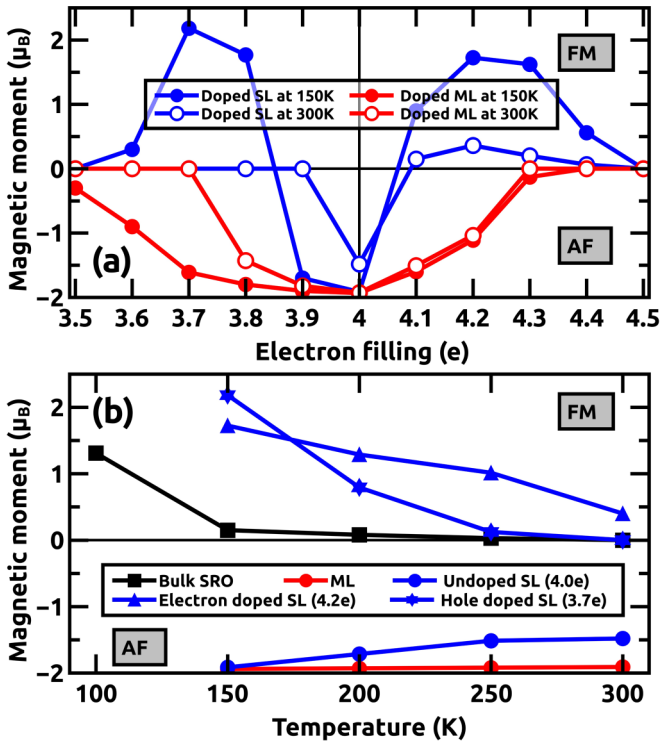

FIG. 3. (Color online) (a) Magnetic moment of SRO monolayer (ML) and $(STO)_5:(SRO)_1$ superlattice (SL) vs doping at 150 and 300 K [positive (negative) moments denote FM (AF) ordering]. (b) Magnetic moments vs temperature for orthorhombic bulk SRO, monolayer, undoped, and doped $(STO)_5:(SRO)_1$ superlattice.

The above calculations reveal that the non-FM insulating state is a robust feature of the SRO monolayer. Only for an unrealistically small U-to-bandwidth ratio can a FM phase be stabilized (see the Supplemental Material). In consequence, the standard manipulation strategies available to the production of thin films can *not* tune this ratio sufficiently to induce ferromagnetism in the SRO monolayer. This stability explains why experimental efforts to create ultrathin ferromagnetic films have so far been unsuccessful.

Doping. Here we propose an alternative route to achieve ultrathin FM films: doping. This strategy may seem counterintuitive at first glance as carrier doping causes a deterioration of the desired properties in the *bulk*. As we shall see, the situation for ultrathin films is different: Using the virtual crystal approximation to simulate carrier doping within DFT+DMFT, we obtain for the SRO monolayer and the $(STO)_5:(SRO)_1$ superlattice the magnetic moments shown in Fig. 3. For the SRO monolayer a significant doping corresponding to 3.5 and 4.5 electrons/site is needed to turn the AF state into a PM at both low (150 K) and high temperature (300 K) [see Fig. 3(a)]. The AF magnetic moment is essentially symmetric around the filling with four electrons. The reason for this is the previously mentioned crystal-field effect that results in an almost fully occupied xy orbital and a half-filled (particle-hole symmetric) yz/xz orbital doublet. We note that, in all cases, the doping away from four electrons induces a metallic state.

Let us now turn to the more important case, the $(STO)_5:(SRO)_1$ superlattice: At low temperatures, e.g., at 150 K as

shown in Fig. 3(a), both hole and electron doping can induce strong FM states. In the case of electron doping (filling>4), the FM state is accompanied by an alternating orbital ordering of the xz/yz minority spin. The spectral function corresponding to 4.3 electrons/site is shown in Fig. 2(b). There, one Ru site has the orbital occupations for up (down) spin, xy 1.00 (0.34), yz 0.97 (0.83), and xz 0.97 (0.19), while for the second Ru site, xy 1.00 (0.34), yz 0.97 (0.19), and xz 0.97 (0.83). For hole doping, e.g., at 3.7 electrons, our DMFT results indicate that the system is a FM half metal with a moment of $2.20\mu_B$/Ru at 150 K [see Fig. 3(b) and the Supplemental Material for the corresponding spectral functions]. The half-metallic behavior makes this setup a prospective candidate for spintronics applications. To put this finding into perspective, we recall that bulk SRO has a FM moment of $2\mu_B$/Ru or less, and an experimental (theoretical) Curie temperature of "only" 160 K (150 K). One might thus wonder whether the ferromagnetism of the doped supercell is actually superior to the hailed properties of stoichiometric bulk SRO, which we were striving to restore. To investigate this, we perform calculations as a function of temperature [see Fig. 3(b)]. We find that for both hole and electron doping, magnetic moments and Curie temperatures of the supercell are remarkably higher than for bulk SRO. In particular, for 4.2 electrons/Ru site, a sizable magnetic moment survives up to room temperature, 300 K [see Fig. 3(b)]. The magnetization curve has a similar shape as for the bulk [49], despite the much higher T_C and the orbital ordering. In the Supplemental Material we also go beyond the virtual crystal approximation and show that a $(STO)_5:(La_{0.25}Sr_{0.75}RuO_3)_1$ superlattice is indeed FM. Our findings pave the road for realizing FM oxide devices that can be operated at room temperature.

Conclusion. Including many-body effects by means of DFT+DMFT, we show that the SRO monolayer is an AF Mott insulator owing to a correlation enhanced crystal-field splitting in the top layer. While the bare (one-particle) crystal-field splitting can be tuned to almost zero by STO capping layers, electronic correlations are still strong enough to boost the orbital separation so that the capped SRO layer also remains an AF insulator. A FM metallic state is only realized for an interaction-to-bandwidth ratio that cannot be achieved by experiment. This explains why ultrathin FM films could not be stabilized in experiment to date. Given the robustness of the AF state of SRO monolayer setups to standard thin-film manipulation techniques, we propose an alternative route to realize a FM state: Our study suggests that carrier doping drives ultrathin SRO films capped with STO into a strong FM state, whose ordered moment and Curie temperature even exceed the values realized in stoichiometric bulk SRO. To achieve the long-standing quest for a FM ultrathin film in practice, we consider inducing oxygen or Sr vacancies [56] or doping potassium into STO:SRO superlattices [23] as the most promising means.

Our study also opens a different, general, perspective: Producing heterostructures based on materials with optimized *bulk* properties (e.g., stoichiometric SRO) is actually not always the optimal way for achieving those properties in a *film* geometry. Indeed, the electronic structure of the thin film is so different from the bulk that it can be viewed as a completely different material. A manipulation (in our case doping) that decreases the quality of the bulk can in fact enhance the sought-after property (FM magnetic moment) for the film setup. This suggests in turn that rather inconspicuous bulk materials might actually be good candidates for specific functionalities when deployed in a film or heterostructure. With this observation, the repertoire of materials to be evaluated for oxide-electronics applications is significantly enlarged.

Acknowledgments. L.S., J.M.T., and K.H. acknowledge financial support by the European Research Council under the European Union's Seventh Framework Program (FP/2007-2013)/ERC through Grant Agreement No. 306447. L.S. also thanks the Austrian Science Fund (FWF) for support through the Doctoral School W1243 Solids4Fun (Building Solids for Function), and Z.Z. acknowledges support by the FWF through the SFB ViCoM F4103. Calculations have been done on the Vienna Scientific Cluster (VSC).

[1] J. Junquera and P. Ghosez, Nature (London) **422**, 506 (2003).

[2] M. Stengel and N. A. Spaldin, Nature (London) **443**, 679 (2006).

[3] H. N. Lee, H. M. Christen, M. F. Chisholm, C. M. Rouleau, and D. H. Lowndes, Appl. Phys. Lett. **84**, 4107 (2004).

[4] C. Eom, R. Cava, R. Fleming, J. M. Phillips, J. Marshall, J. Hsu, J. Krajewski, W. Peck *et al.*, Science **258**, 1766 (1992).

[5] G. Koster, L. Klein, W. Siemons, G. Rijnders, J. S. Dodge, C.-B. Eom, D. H. Blank, and M. R. Beasley, Rev. Mod. Phys. **84**, 253 (2012).

[6] T. Kiyama, K. Yoshimura, K. Kosuge, Y. Ikeda, and Y. Bando, Phys. Rev. B **54**, R756 (1996).

[7] G. Cao, S. McCall, M. Shepard, J. E. Crow, and R. P. Guertin, Phys. Rev. B **56**, 321 (1997).

[8] P. B. Allen, H. Berger, O. Chauvet, L. Forro, T. Jarlborg, A. Junod, B. Revaz, and G. Santi, Phys. Rev. B **53**, 4393 (1996).

[9] I. Felner, K. Nomura, and I. Nowik, Phys. Rev. B **73**, 064401 (2006).

[10] Z. Fang, N. Nagaosa, K. S. Takahashi, A. Asamitsu, R. Mathieu, T. Ogasawara, H. Yamada, M. Kawasaki, Y. Tokura, and K. Terakura, Science **302**, 92 (2003).

[11] M. S. Laad and E. Müller-Hartmann, Phys. Rev. Lett. **87**, 246402 (2001).

[12] P. Werner, E. Gull, M. Troyer, and A. J. Millis, Phys. Rev. Lett. **101**, 166405 (2008).

[13] D. Jeong, H. C. Choi, C. H. Kim, S. H. Chang, C. Sohn, H. Park, T. Kang, D.-Y. Cho, S. Baek, C. Eom *et al.*, Phys. Rev. Lett. **110**, 247202 (2013).

[14] D. E. Shai, C. Adamo, D. W. Shen, C. M. Brooks, J. W. Harter, E. J. Monkman, B. Burganov, D. G. Schlom, and K. M. Shen, Phys. Rev. Lett. **110**, 087004 (2013).

[15] D. Toyota, I. Ohkubo, H. Kumigashira, M. Oshima, T. Ohnishi, M. Lippmaa, M. Takizawa, A. Fujimori, K. Ono, M. Kawasaki *et al.*, Appl. Phys. Lett. **87**, 162508 (2005).

[16] D. Toyota, I. Ohkubo, H. Kumigashira, M. Oshima, T. Ohnishi, M. Lippmaa, M. Kawasaki, and H. Koinuma, J. Appl. Phys. **99**, 08N505 (2006).
[17] J. Xia, W. Siemons, G. Koster, M. R. Beasley, and A. Kapitulnik, Phys. Rev. B **79**, 140407 (2009).
[18] Y. J. Chang, C. H. Kim, S.-H. Phark, Y. S. Kim, J. Yu, and T. W. Noh, Phys. Rev. Lett. **103**, 057201 (2009).
[19] M. Verissimo-Alves, P. García-Fernández, D. I. Bilc, P. Ghosez, and J. Junquera, Phys. Rev. Lett. **108**, 107003 (2012).
[20] K. Gupta, B. Mandal, and P. Mahadevan, Phys. Rev. B **90**, 125109 (2014).
[21] J. M. Rondinelli, N. M. Caffrey, S. Sanvito, and N. A. Spaldin, Phys. Rev. B **78**, 155107 (2008).
[22] P. Mahadevan, F. Aryasetiawan, A. Janotti, and T. Sasaki, Phys. Rev. B **80**, 035106 (2009).
[23] F. Bern, M. Ziese, A. Setzer, E. Pippel, D. Hesse, and I. Vrejoiu, J. Phys.: Condens. Matter **25**, 496003 (2013).
[24] V. J. Emery and S. A. Kivelson, Phys. Rev. Lett. **74**, 3253 (1995).
[25] A. Georges, G. Kotliar, W. Krauth, and M. J. Rozenberg, Rev. Mod. Phys. **68**, 13 (1996).
[26] G. Kotliar and D. Vollhardt, Phys. Today **57** (3), 53 (2004).
[27] K. Held, Adv. Phys. **56**, 829 (2007).
[28] V. I. Anisimov, F. Aryasetiawan, and A. Lichtenstein, J. Phys.: Condens. Matter **9**, 767 (1997).
[29] G. Kotliar, S. Y. Savrasov, K. Haule, V. S. Oudovenko, O. Parcollet, and C. Marianetti, Rev. Mod. Phys. **78**, 865 (2006).
[30] C. Jones, P. Battle, P. Lightfoot, and W. Harrison, Acta Crystallogr., Sect. C **45**, 365 (1989).
[31] K. Momma and F. Izumi, J. Appl. Crystallogr. **44**, 1272 (2011).
[32] G. Kresse and J. Hafner, Phys. Rev. B **48**, 13115 (1993).
[33] G. Kresse and J. Furthmüller, Comput. Mater. Sci. **6**, 15 (1996).
[34] J. P. Perdew, K. Burke, and M. Ernzerhof, Phys. Rev. Lett. **77**, 3865 (1996).
[35] P. Blaha, K. Schwarz, G. Madsen, D. Kvasnicka, and J. Luitz, *WIEN2K: An Augmented Plane Wave+Local Orbitals Program for Calculating Crystal Properties* (Univ. Prof. Dr. Karlheinz Schwarz, Techn. Universität Wien, Vienna, 2001).
[36] F. Tran and P. Blaha, Phys. Rev. Lett. **102**, 226401 (2009).
[37] As detailed in the Supplemental Material, the exchange included in mBJ does not notably affect the t_{2g} bandwidth, but it improves on the interorbital separation for states not included in the DMFT. It is in this sense a "poor man's version" of the QSGW+DMFT approach that combines quasi-particle self-consistent (QS) *GW* with DMFT [57].
[38] N. Marzari, A. A. Mostofi, J. R. Yates, I. Souza, and D. Vanderbilt, Rev. Mod. Phys. **84**, 1419 (2012).
[39] A. A. Mostofi, J. R. Yates, Y.-S. Lee, I. Souza, D. Vanderbilt, and N. Marzari, Comput. Phys. Commun. **178**, 685 (2008).
[40] J. Kuneš, R. Arita, P. Wissgott, A. Toschi, H. Ikeda, and K. Held, Comput. Phys. Commun. **181**, 1888 (2010).
[41] N. Parragh, A. Toschi, K. Held, and G. Sangiovanni, Phys. Rev. B **86**, 155158 (2012).
[42] E. Gull, A. J. Millis, A. I. Lichtenstein, A. N. Rubtsov, M. Troyer, and P. Werner, Rev. Mod. Phys. **83**, 349 (2011).
[43] F. Aryasetiawan, M. Imada, A. Georges, G. Kotliar, S. Biermann, and A. I. Lichtenstein, Phys. Rev. B **70**, 195104 (2004); T. Miyake and F. Aryasetiawan, *ibid.* **77**, 085122 (2008).
[44] Z. Zhong, M. Wallerberger, J. M. Tomczak, C. Taranto, N. Parragh, A. Toschi, G. Sangiovanni, K. Held, Phys. Rev. Lett. **114**, 246401 (2015),
[45] H. Hadipour and M. Akhavan, Eur. Phys. J. B **84**, 203 (2011).
[46] E. Jakobi, S. Kanungo, S. Sarkar, S. Schmitt, and T. Saha-Dasgupta, Phys. Rev. B **83**, 041103 (2011).
[47] O. Grånäs, I. Di Marco, O. Eriksson, L. Nordström, and C. Etz, Phys. Rev. B **90**, 165130 (2014).
[48] D. J. Singh, J. Appl. Phys. **79**, 4818 (1996).
[49] M. Kim and B. Min, Phys. Rev. B **91**, 205116 (2015).
[50] K. Ishigami, K. Yoshimatsu, D. Toyota, M. Takizawa, T. Yoshida, G. Shibata, T. Harano, Y. Takahashi, T. Kadono, V. Verma *et al.*, arXiv:1505.05692.
[51] See Supplemental Material at http://link.aps.org/supplemental/10.1103/PhysRevB.92.041108 for a further details of the calculations, spectral functions of all considered setups, and quantitative information on the correlation enhanced crystal-field splittings.
[52] A. I. Poteryaev, M. Ferrero, A. Georges, and O. Parcollet, Phys. Rev. B **78**, 045115 (2008).
[53] G. Keller, K. Held, V. Eyert, D. Vollhardt, and V. I. Anisimov, Phys. Rev. B **70**, 205116 (2004).
[54] A. I. Poteryaev, J. M. Tomczak, S. Biermann, A. Georges, A. I. Lichtenstein, A. N. Rubtsov, T. Saha-Dasgupta, and O. K. Andersen, Phys. Rev. B **76**, 085127 (2007).
[55] W. Tian, J. Haeni, D. Schlom, E. Hutchinson, B. Sheu, M. Rosario, P. Schiffer, Y. Liu, M. Zurbuchen, and X. Pan, Appl. Phys. Lett. **90**, 022507 (2007).
[56] J. Kim, J. Chung, and S.-J. Oh, Phys. Rev. B **71**, 121406 (2005).
[57] J. M. Tomczak, J. Phys.: Conf. Ser. **592**, 012055 (2015); C. Taranto, M. Kaltak, N. Parragh, G. Sangiovanni, G. Kresse, A. Toschi, and K. Held, Phys. Rev. B **88**, 165119 (2013).